

*Original Research*

# Efficiency Improvement through Electro-Spraying Process of Hybrid SiO<sub>2</sub>-VO<sub>2</sub> Anti-Reflection Coating for Monocrystalline Silicon Photovoltaic Cells

Naser A. Alsaleh <sup>1,\*</sup><sup>1</sup> Industrial Engineering Department, College of Engineering, Imam Mohammad Ibn Saud Islamic University (IMSIU), Riyadh 11432, Saudi Arabia

\* Correspondence: naalsaleh@imamu.edu.sa

Received: December 15, 2025; Accepted: January 19, 2026

**Abstract:** Utilizing the incident solar radiation into electrical energy through monocrystalline silicon solar cells has recently gained great interest in the field of advanced manufacturing. Reflection loss is a critical optical loss affecting solar cells performance. Through the process of antireflection coating, some of the scattered incident photons could be transmitted into the solar cells which leads to better utilization of incident light rays and improves efficiency. In the present work, antireflective materials such as SiO<sub>2</sub>, VO<sub>2</sub> and SiO<sub>2</sub>-VO<sub>2</sub> mixture films were coated over the silicon solar cell through an electro-spraying process. Characterization techniques such as XRD, AFM and FESEM were exploited to evaluate the efficiency of the electro-spraying process through the film's crystalline properties, agglomeration formation and surface property of the films formed over the solar cells. The results demonstrated that SiO<sub>2</sub>-VO<sub>2</sub> blended solar cell showed a minimum reflectance of 6.55% compared to bare cell. After coating the solar cell with SiO<sub>2</sub>-VO<sub>2</sub>, it exhibited higher power conversion efficiency of 24.87% under regulated environment. It acquires the narrow length of visible spectrum and serves as a yellow/green filter in visible spectrum. This electro-spraying process improves the capability of the cells to transmit the light as in sunlight with uniform radiation. It increased the photon transmission which reached the depletion region. The minimum resistivity of  $5.37 \times 10^{-3} \Omega \cdot \text{cm}$  was achieved when the electro-spraying process applies a film of SiO<sub>2</sub>-VO<sub>2</sub> blend on the cell, which is lower than all other samples. The electro-spraying process of SiO<sub>2</sub>-VO<sub>2</sub> blend decreased reflection by reducing sunlight scattering.

**Keywords:** electro-spraying process; advanced manufacturing; antiglare coatings; monocrystalline Si solar cells; renewable energy

---

## 1. Introduction

Sunlight can be utilised as electrical energy, heat energy and hybridised chemical energy. Some of the solar energy conversion devices were PV cells, thermal collector devices and solar-chemical devices. In all these devices, energy conversion was affected mainly due to the surface reflection. Around 5–10 % of incident solar light gets reflected back from the solar cell surface resulting in the 9–14 % decrease in the solar energy conversion into electrical or heat energy, more specifically in the visible spectrum [1]. Anti-glare surface coatings were key factors for the overcoming the light reflection due to optical losses. By the proper selection and coating of anti-glare layers with refractive index lying better the optimal working range, some scattering photons can be trapped and been transmitted into the depletion layer of solar cell [2]. Conventional antireflection coating was implemented in single or multilayer thin films either with single or multiple materials. It is usually a dielectric material with transparent nature, which holds refractive index between the specified

range [3]. The anti-glare coatings were performed through various techniques such as physical and chemical vapour deposition and sol gel synthesis. However, these techniques were preferred in laboratory scale due to its high equipment cost, complex operating environment and low scale operation.

Further, micro and nano texturing of silicon substrates has also become a trending technology of reducing reflection and maximizing trapping of light in photovoltaic devices alongside the thin-film antireflection coatings. Such texturing techniques create irregular or pyramidal features, surface structures, which permit multiple interior reflections and improvement of the optical path length and absorbs photon within the active layer [4]. Etching micro-pyramid alkaline and metal-assisted chemical etching (MACE) nanoscale structure have all demonstrated the capability to reduce surface reflectivity to less than 10% at the entire solar light wave length range [5]. The optical performance of the textured surface with antireflection coating is superior to that of individual methods in that, the textured surface has the benefit of geometrical light trapping and coating work on the gradient of the refractive index. However, the texturing processes may be expensive to the other chemical treatments, sensitive to control of the etching parameters, and may cause surface defects or significant recombination losses unless passivated. Therefore, the development of cost effective, standardized processes of coating such as electro-spraying is highly crucial in increasing the effectiveness of solar cells in large scale manufacturing.

As seen, some of the large-scale anti-glare thin film coating can be obtained through blade coating, knife edge coating, brush coating, screen printing etc., Uniform and good adherence of coated films cannot be achieved easily [6]. This drawback can be overcome through electro spraying coating technique. The setup has syringe with needle loaded with the coating material dispersed with ethanol. High voltage supply, preset mass flow rate, spinneret velocity, plate velocity and distance between the needle and plate were the crucial operating parameters. The coating was performed by charging the needle tip with positive charge and deposition plate with negative charge separated at very small distance [7]. With the influence of strong electrostatic force of attraction, the ejected coating material gets split into finer droplets and gets adhered over the plate surface. This coating technique can be performed under atmospheric temperature and pressure which make it as low -cost operation resulting in better morphology and control over coating thickness. It is mainly suited for hybrid material coating over selected substrates [8].

Combined effect of two anti-reflective materials with refractive index closer to each other showed better photon transmission and declined reflectance resulting in elevated performance of solar cell. Also, blended anti-glare materials exerts long term sustainability. The present works, as illustrated in Figure 1, aims to utilise the thin film transparent antiglare coatings of SiO<sub>2</sub>, VO<sub>2</sub> and SiO<sub>2</sub>-VO<sub>2</sub> mechanical blends through electro-spray technique [9]. The power output performance of purchased, SiO<sub>2</sub>, VO<sub>2</sub>, SiO<sub>2</sub>-VO<sub>2</sub> blended solar cells were evaluated through variety of characterisation techniques. Some of the inspection methods for determining the optical, structural, electrical, thermal and morphological studies through FESEM, AFM, Four -probe method, IR thermal imaging, UV-Vis spectroscopy. With the optimal coating parameters, the anti-glare coatings hold progressive optical performance in addition to thermal performance. Thus, blended antireflection coating found to be promising antireflection layer capable of delivering the high-power output with subsequent reduction in optical reflectance. Antireflection coatings made of oxides can as well lead to long term reliability of photovoltaic devices. The silicon surface is shielded against the infiltration of moisture and contaminants in the air by the SiO<sub>2</sub>-VO<sub>2</sub> layer creating a dense and smooth shield. This protection is effective in reducing the degradation at the surface as well as stabilizing electrical characteristics in the long runs of illumination. Also, the thermal and chemical stability of oxide coating promotes performance stability in the operating conditions. These properties show that the coating applied is not only efficient, but also increases the reliability of devices [10].

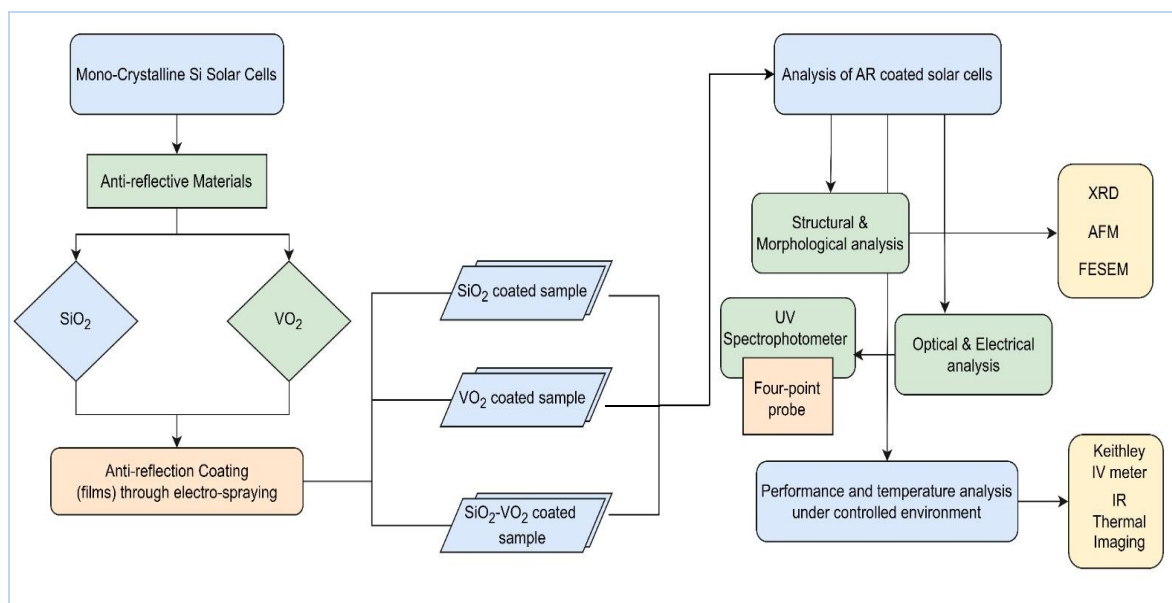


Figure 1. Flowchart of research workflow.

## 2. Materials and Methods

### 2.1. Materials

The Monocrystalline silicon solar cells of dimensions 38×52 mm (obtained from Vikram Solar) were used for the investigation. SiO<sub>2</sub> and VO<sub>2</sub> and Ethanol with 99.9% purity (provided by Spectrum Reagents and Chemicals Pvt. Ltd.) were also used as reflective coating materials. A 99.9% pure Ethanol (a product of Herenba Instruments and Engineers) was used as blending medium.

### 2.2. SiO<sub>2</sub>-VO<sub>2</sub> Blend Mixture Preparation

SiO<sub>2</sub>-VO<sub>2</sub> blend was prepared using ball milling technique which was found to be more effective for the preparation of homogenous mixture. This technique also helps to reduce the particle size. With the help of planetary ball mill, the materials were mixed together under normal atmosphere for up to 240 minutes. This prolonged process led to the formation of different metastable phases resulting in the better mixing of selected anti-glare materials. The rotational speed was maintained as 1500 rpm. Finally, the prepared mixture was collected and thoroughly washed using deionised water and followed by alcohol. The washed homogenous mixture was then dried in hot air oven at 75 °C.

### 2.3. SiO<sub>2</sub>-VO<sub>2</sub> Blend Mixture Coating

The prepared SiO<sub>2</sub>-VO<sub>2</sub> mixture was taken in the beaker along with 100 ml of ethanol. Afterwards, it was thoroughly mixed using magnetic stirrer for 40 minutes. The obtained mixture was sonicated using ultrasonicator. The sonication process was performed for 30 minutes resulting in deagglomeration of mixture particles. Lastly, the obtained mixture was loaded into the 5 ml syringe with a spraying tip. With the pre-set mass flow rate, the syringe was pressed and the dispersed fluid was ejected and sprayed out in very finer droplets. Because of the electrohydrodynamic atomisation, the ejected droplets were deposited over the solar cells leading to uniform deposition, through electro-spraying. The coating was performed for SiO<sub>2</sub>, VO<sub>2</sub> and SiO<sub>2</sub>-VO<sub>2</sub> mechanical blends over the solar cell surface by the use of the same electro-spraying process.

#### 2.4. Characterization Methods to Analyse the Anti-reflective Materials Coated Solar Cell

Different characterization methods were employed to evaluate the efficiency of bare cell and the  $\text{SiO}_2$ ,  $\text{VO}_2$ , and  $\text{SiO}_2\text{-VO}_2$  coated photovoltaic samples by the electro-spraying process. X-Ray Diffraction was used to characterize the phase and crystalline nature of the solar cell samples. Field Emission Scanning Electron Microscopy (FESEM) was performed using a ZEISS GEMINI SEM 500 (Carl Zeiss, Germany) to investigate the cross-section and surface morphologies of the solar cells. Atomic Force Microscopy was used in tapping mode under atmospheric condition for analysing the surface roughness of bare and coated cell. UV-visible absorption spectra were recorded using a Shimadzu UV-1800 and UV-visible spectrophotometer (Shimadzu Corp., Japan) was employed for recording the reflectance spectra in the wavelength between 300–1200 nm. Four-point probe technique was used to measure the electrical properties such as resistivity, hall mobility and carrier concentration of the solar cells. A Keithley 2400 SourceMeter® (Keithley Instruments Inc., USA) was employed for I-V measurements to measure the photocurrent-voltage parameters like current density, open-circuit voltage and fill factor of the photovoltaic samples. The cell temperature of bare cell,  $\text{SiO}_2$ ,  $\text{VO}_2$  and  $\text{SiO}_2\text{-VO}_2$  coated samples were measured using Infra-Red Thermal Imaging technique [11].

### 3. Results and Discussions

#### 3.1. XRD Analysis

The crystal arrangement and position of pure  $\text{SiO}_2$ ,  $\text{VO}_2$ , and  $\text{SiO}_2\text{-VO}_2$  coated by the electro-spraying process on a Silicon photovoltaic substrate is analysed using XRD and shown in Figure 2. There is a silicon peak could be found, that is because the anti-reflective materials like  $\text{SiO}_2$  and  $\text{VO}_2$  coated on a Si surface. As illustrated in XRD peaks of Figure 2,  $\text{VO}_2$  on Si substrate affirmed only monoclinic diffraction pattern. The  $\text{SiO}_2\text{-VO}_2$  peaks exhibited a single-phase  $\text{VO}_2$  and the peaks were sharp. Hence, it is proved that the  $\text{SiO}_2$  with higher amorphous was found. No peaks of any other phases or impurities were found, showing the higher level of purity of the coating materials [12]. The average size of the crystallite and width of the peaks were correlated. Various parts of the sample were evaluated and exhibited the same properties, demonstrating the uniformity in their crystallization and composition.

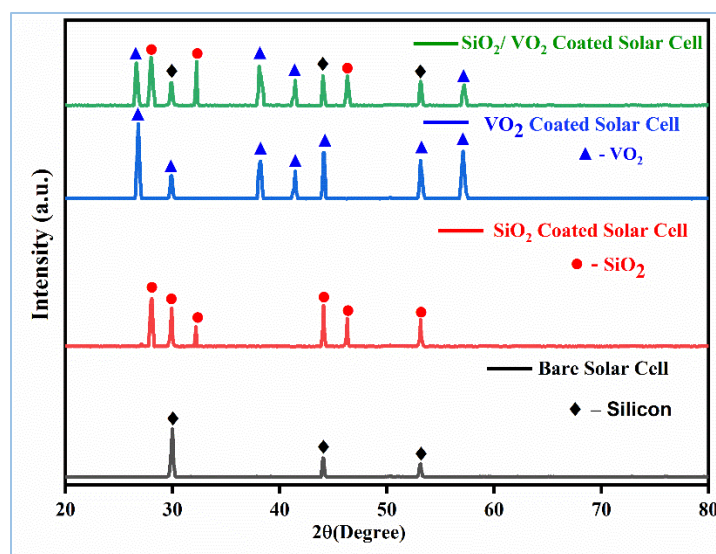


**Figure 2.** XRD of  $\text{SiO}_2\text{-VO}_2$  coated over silicon solar cell by the electro-spraying process.

### 3.2. Surface Roughness Analysis

Figure 3 illustrates the surface roughness images of SiO<sub>2</sub> and VO<sub>2</sub> films coated by the electro-spraying process. The AFM analysis was performed under atomic force microscope (Dimension Icon, Bruker, USA) to evaluate the regularity of materials on coated substrates and to understand the coating thickness. The surface roughness of SiO<sub>2</sub>, VO<sub>2</sub> and SiO<sub>2</sub>-VO<sub>2</sub> is observed as 38 nm, 44 nm and 50 nm. The particle agglomeration, grain refinement and grain growth were observed. For the SiO<sub>2</sub>-VO<sub>2</sub> coating film, the AFM morphology gives a comparably fine-granulated microstructure. The size distribution of the particles differs from 30 to 70 nm, demonstrating the increased uniform surface morphology. Disregarding of the less variation in surface roughness, SiO<sub>2</sub> and VO<sub>2</sub> coatings firmly attach to the Si surface, thus promoting the sunlight propagation [13]. The SiO<sub>2</sub>, VO<sub>2</sub> and SiO<sub>2</sub>-VO<sub>2</sub> films displayed an impenetrable structure having higher thickness therefore improving their capacity to efficiently trap the reflected photons.

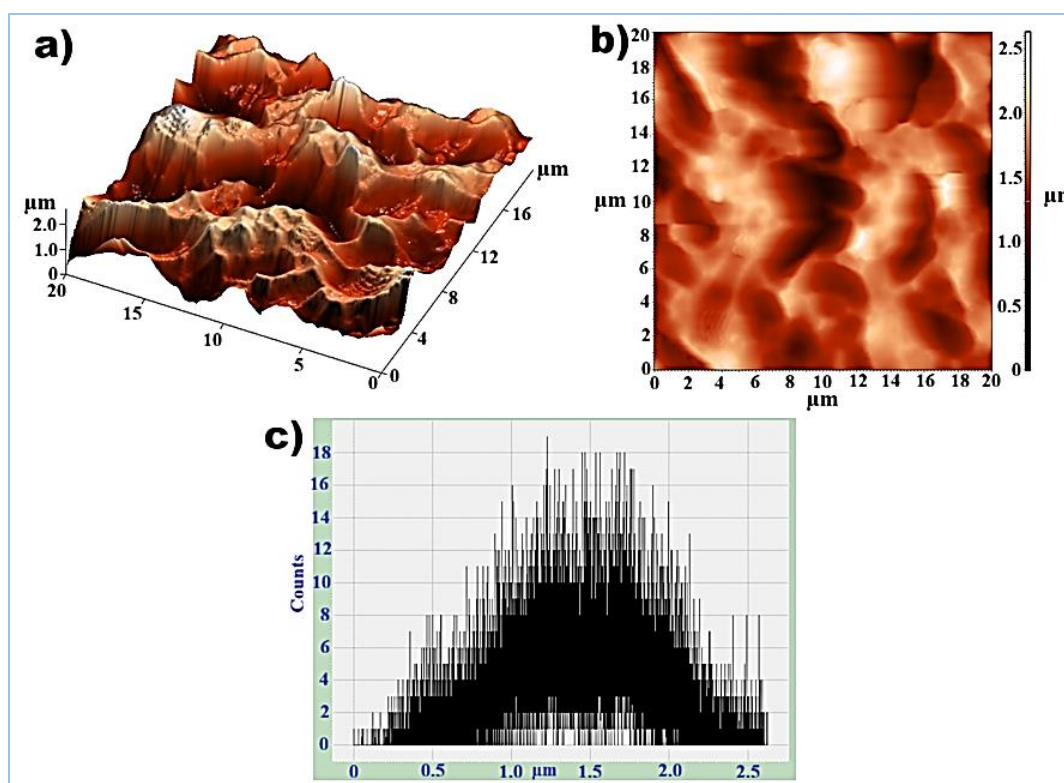


**Figure 3.** Morphology of AFM of SiO<sub>2</sub>-VO<sub>2</sub> blend coated solar cell by the electro-spraying process. (a) 3D topography; (b) 2D topography; (c) Histogram analysis.

### 3.3. FESEM Analysis

The sectional view and morphological characteristics of the samples were evaluated using FESEM method. The SEM images of SiO<sub>2</sub>, VO<sub>2</sub> and SiO<sub>2</sub>-VO<sub>2</sub> coated on the photovoltaic cells by the electro-spraying process were shown in Figure 4. The coatings have optically dense structure. The thicknesses of the SiO<sub>2</sub>, VO<sub>2</sub> and SiO<sub>2</sub>-VO<sub>2</sub> films were found as to be 223 nm, 303 nm and 390 nm, respectively. The SiO<sub>2</sub>-VO<sub>2</sub> coating exhibited a fine structure having well-proportioned grains homogeneously growing over the entire Si photovoltaic surface as seen in Figure 4. The particle clusters formation and interconnected pores were observed among particles and smooth surface observed across the particle surface. As shown in Figure 4, the surface of SiO<sub>2</sub> and VO<sub>2</sub> film is uniform and compact with grain size. The substrate to nozzle distance, voltage supply and rate of flow were

the factors which affects the coating's quality. The surface defects were not found in the samples. Certainly, the smooth and even surface achieved by the electro-spraying process of SiO<sub>2</sub>-VO<sub>2</sub> film improved the absorption of sunlight in active sites and consequently increases the absorption ability [14]. The electro sprayed materials were completely attached with the frontal area of solar cell because of strong electrostatic attractive force.

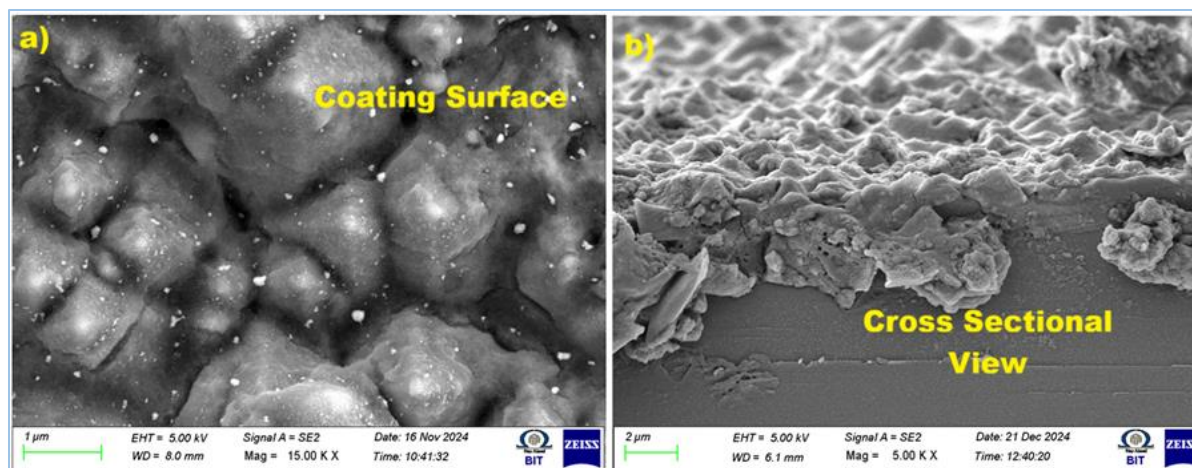


**Figure 4.** FESEM of blended SiO<sub>2</sub>-VO<sub>2</sub> coated solar cell by the electro-spraying process. (a) Surface morphology; (b) Cross-sectional view.

### 3.4. Optical Reflectance and Quantum Efficiency Analysis

In Figure 5 reflectance curve and External Quantum efficiency (EQE) is illustrated for bare cell, SiO<sub>2</sub>, VO<sub>2</sub> and SiO<sub>2</sub>-VO<sub>2</sub> coated photovoltaic samples. UV Visible spectroscopy was employed for measuring the optical property like reflectance of the solar cells. The reflectance value of bare cell, SiO<sub>2</sub>, VO<sub>2</sub> and SiO<sub>2</sub>-VO<sub>2</sub> coated cell were measured as 16.36%, 12.17%, 10.24% and 6.55%, respectively. The reflection values are reduced after coating by the electro-spraying process using antireflective materials as shown in Figure 5. Compared to all samples, blended SiO<sub>2</sub>-VO<sub>2</sub> showed minimum reflectance. The absorbed electrons per incident photons gives the External Quantum efficiency. The External Quantum efficiency data showed that the electrons and photons combined with photovoltaic surface. The SiO<sub>2</sub>-VO<sub>2</sub> coated solar cell sample exhibited the highest quantum efficiency as compared to other samples. The quantum efficiency values for bare cell, SiO<sub>2</sub>, VO<sub>2</sub> and SiO<sub>2</sub>-VO<sub>2</sub> was measured as 80.17%, 85.71%, 91.09% and 96.45%, respectively. It is due to the minimum reflection of incident rays in the photovoltaic cell. The rough surface and ideal coating thickness increased the light propagation and decreased the light scattering [15]. The existence of Silicon and Vanadium facilitated more sunlight to penetrate through the solar cells. Table 1 gives the summary of reflectance and EQE data analysed using UV spectroscopy. In order to have optimum antireflection on silicon the refractive index of the coating would ideally between  $n \approx 1.9-2.0$ . The refractive index of the materials used separately is SiO<sub>2</sub> ( $n \approx 1.46$ ) and VO<sub>2</sub> ( $n \approx 2.8$ ), which are not in the close range of this ideal value. The VO<sub>2</sub> mixture in SiO<sub>2</sub> introduces a more realistic range of refractive index ( $n \approx 1.8-2.2$ ) that lies much closer to the optimum range and provides much closer matching impedance between silicon and air. This is why the blended coating presents the least reflectance (6.55%) as compared to that of SiO<sub>2</sub> (12.17%) and VO<sub>2</sub> (10.24%).

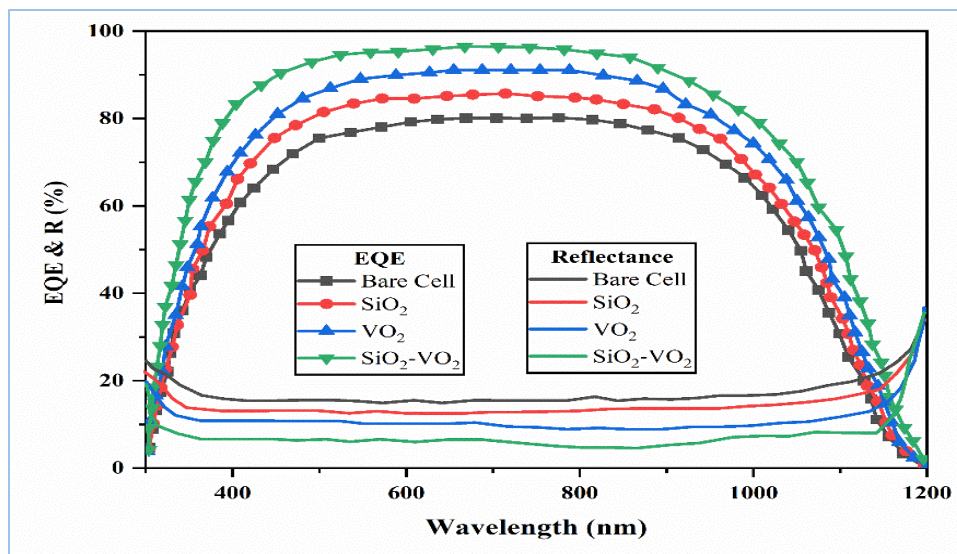


Figure 5. Optical reflectance and EQE curve of bare, SiO<sub>2</sub>, VO<sub>2</sub> and blended SiO<sub>2</sub>-VO<sub>2</sub> coated cell using the electro-spraying process.

Table 1. Reflectance and EQE measurements of bare cell, SiO<sub>2</sub>, VO<sub>2</sub> and SiO<sub>2</sub>-VO<sub>2</sub> coated solar cells.

Specimen	Reflectance (%)	EQE (%)
Bare cell	16.36	80.17
SiO <sub>2</sub>	12.17	85.71
VO <sub>2</sub>	10.24	91.09
Blended SiO <sub>2</sub> -VO <sub>2</sub>	6.55	96.45

### 3.5. Performance Analysis in Regulated Environment

The efficiency of solar cell is measured under a controlled environment employing solar simulator. The evaluated photocurrent–voltage property of the solar cell is shown in Figure 6. The efficiency characteristics of coated solar cell using the electro-spraying process, that are extracted from the I–V graph, are summarized in Table 2. With the anti-reflection coating of SiO<sub>2</sub>, VO<sub>2</sub> and SiO<sub>2</sub>-VO<sub>2</sub>, the power conversion efficiency of solar cell is increased from 17.22% to 24.87%. The enhancement is primarily because of the increased short-circuit current and open-circuit voltage. There is a decrease in efficiency of 17.22% for bare cell with other parameters like  $J_{sc} = 35.75 \text{ mA/cm}^2$ ,  $V_{oc} = 0.61 \text{ V}$  and Fill factor = 74%, respectively. The single material such as SiO<sub>2</sub> and VO<sub>2</sub> coated cells exhibited a power conversion efficiency of 19.99% and 20.76%, respectively. In comparison with all other samples, the blended SiO<sub>2</sub>-VO<sub>2</sub> coated sample provided the maximum efficiency of 24.87% with increased  $J_{sc}$  of  $44.92 \text{ mA/cm}^2$ ,  $V_{oc}$  of 0.692 V and improved FF of 80, respectively. The enhancement in efficiency is because of the transmitted sunlight is transformed more effectively in solar cells. Thus, decreased reflectance could have higher effect on overall efficiency in solar cells [16]. Even though the reduction of the optical reflections is directly proportional to the enhancement of the  $J_{sc}$ , the increment of the  $V_{oc}$  and FF is attributed to other electrical improvements by the antireflection coating. The electro-sprayed SiO<sub>2</sub>-VO<sub>2</sub> film also reduces the surface recombination by formation of smooth and dense interface resulting in improved quality of the junction. Besides, the surface passivation effect, decrease in series resistance, and an enhancement of the hall mobility can enhance the efficiency of charge carrier transport. The combination of these effects leads to a reduced loss in recombination and results in increased  $V_{oc}$ , FF and  $J_{sc}$  [17].

**Table 2.** Photocurrent-voltage results of bare cell, SiO<sub>2</sub>, VO<sub>2</sub> and blended SiO<sub>2</sub>-VO<sub>2</sub> coated solar cell by the electro-spraying process under regulated environment.

Sample	J <sub>sc</sub> (mA/cm <sup>2</sup> )	V <sub>oc</sub> (V)	FF (%)	PCE (%)
Bare cell	35.75	0.651	74	17.22
SiO <sub>2</sub>	39.67	0.663	76	19.99
VO <sub>2</sub>	40.06	0.673	77	20.76
SiO <sub>2</sub> -VO <sub>2</sub>	44.92	0.692	80	24.87

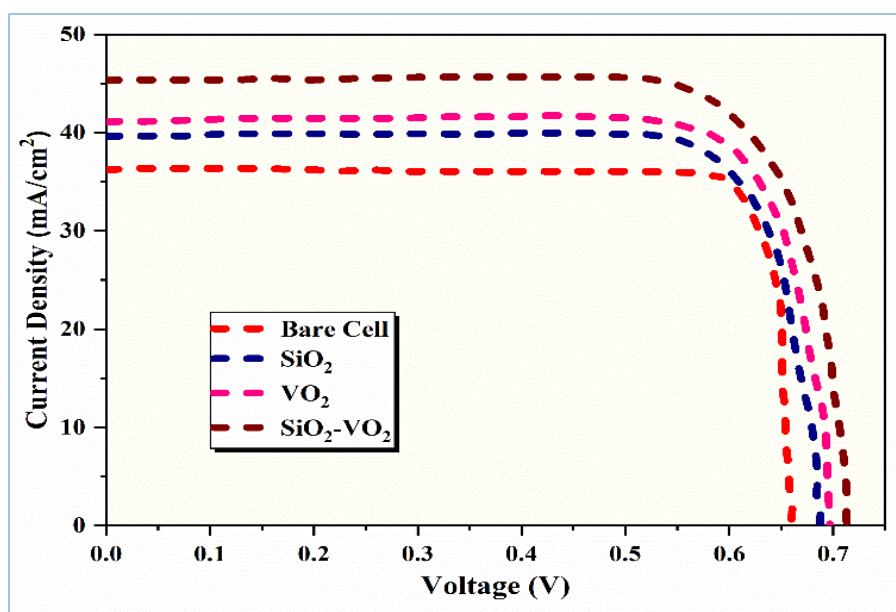


**Figure 6.** I-V graph of bare, SiO<sub>2</sub>, VO<sub>2</sub> and blended SiO<sub>2</sub>-VO<sub>2</sub> coated cell by the electro-spraying process.

### 3.6. Electrical Analysis

The electrical properties of bare, SiO<sub>2</sub>, VO<sub>2</sub> and SiO<sub>2</sub>-VO<sub>2</sub> coated cell using the electro-spraying process were measured using four-probe technique as illustrated in Figure 7. The resistivities of bare, SiO<sub>2</sub>, VO<sub>2</sub> and SiO<sub>2</sub>-VO<sub>2</sub> coated sample were measured as  $9.23 \times 10^{-3} \Omega \cdot \text{cm}$ ,  $8.44 \times 10^{-3} \Omega \cdot \text{cm}$ ,  $6.76 \times 10^{-3} \Omega \cdot \text{cm}$  and  $5.37 \times 10^{-3} \Omega \cdot \text{cm}$ , respectively. It is clear that bare cell exerts more resistivity than SiO<sub>2</sub>-VO<sub>2</sub> coated cell. It is primarily because of increased size of grains and lower grain boundaries. It is proved that when the layers of ARC increases, the resistivity decreases, finally lead to increased conductivity in SiO<sub>2</sub> and VO<sub>2</sub> coated photovoltaic sample and also improves mobility of electrons. The carrier concentration of various ARC coated samples varies from  $25.48 \times 10^{20}$  to  $37.36 \times 10^{20} \text{ cm}^{-3}$ . The hall mobility also increased from  $11.22 \text{ cm}^2/\text{Vs}$  to  $15.35 \text{ cm}^2/\text{Vs}$  for bare cell to blended SiO<sub>2</sub>-VO<sub>2</sub> coated cell. When compared to other solar sample, the photo-generated current and conductivity is increasing for double layer coated cell. Table 3 shows the measurements of electrical parameters.

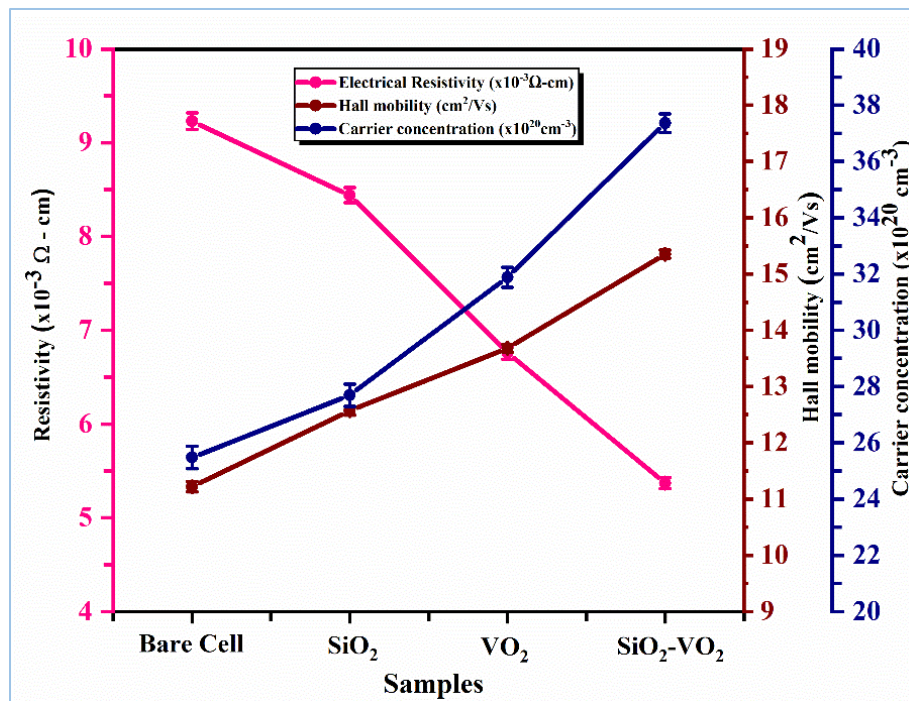


**Figure 7.** Electrical resistivity, carrier concentration and hall mobility analysis curve of bare, SiO<sub>2</sub>, VO<sub>2</sub> and blended SiO<sub>2</sub>-VO<sub>2</sub> coated solar cells by the electro-spraying process.

**Table 3.** Electrical resistivity, carrier concentration and hall mobility of bare, SiO<sub>2</sub>, VO<sub>2</sub> and blended SiO<sub>2</sub>-VO<sub>2</sub> coated Si solar cells the electro-spraying process.

Samples	Resistivity ( $\Omega\text{-cm}$ )	Carrier concentration ( $\text{cm}^{-3}$ )	Hall mobility ( $\text{cm}^2 \text{V}^{-1}\text{s}^{-1}$ )
Bare cell	$9.23 \times 10^{-3}$	$25.48 \times 10^{20}$	11.22
SiO <sub>2</sub>	$8.44 \times 10^{-3}$	$27.69 \times 10^{20}$	12.57
VO <sub>2</sub>	$6.76 \times 10^{-3}$	$31.88 \times 10^{20}$	13.68
SiO <sub>2</sub> -VO <sub>2</sub>	$5.37 \times 10^{-3}$	$37.36 \times 10^{20}$	15.35

### 3.7. Cell Temperature Analysis in Controlled Atmosphere

The efficiency of solar cell is primarily affected by the cell temperature. The performance of solar cell decreases as the cell temperature increases. The power production in photovoltaic cells is also affected by increased resistivity because of increased heat flux [18]. In controlled environment, the temperature of bare cell, SiO<sub>2</sub>, VO<sub>2</sub> and SiO<sub>2</sub>-VO<sub>2</sub> coated cell by the electro-spraying process were measured. An IR thermal imager combined and presented both IR and visible images to a single image as illustrated in Figure 8. It is clear from the Figure 8, that the blended SiO<sub>2</sub>-VO<sub>2</sub> coated cell exhibited lower cell temperature of 41.9°C when compared to bare cell.

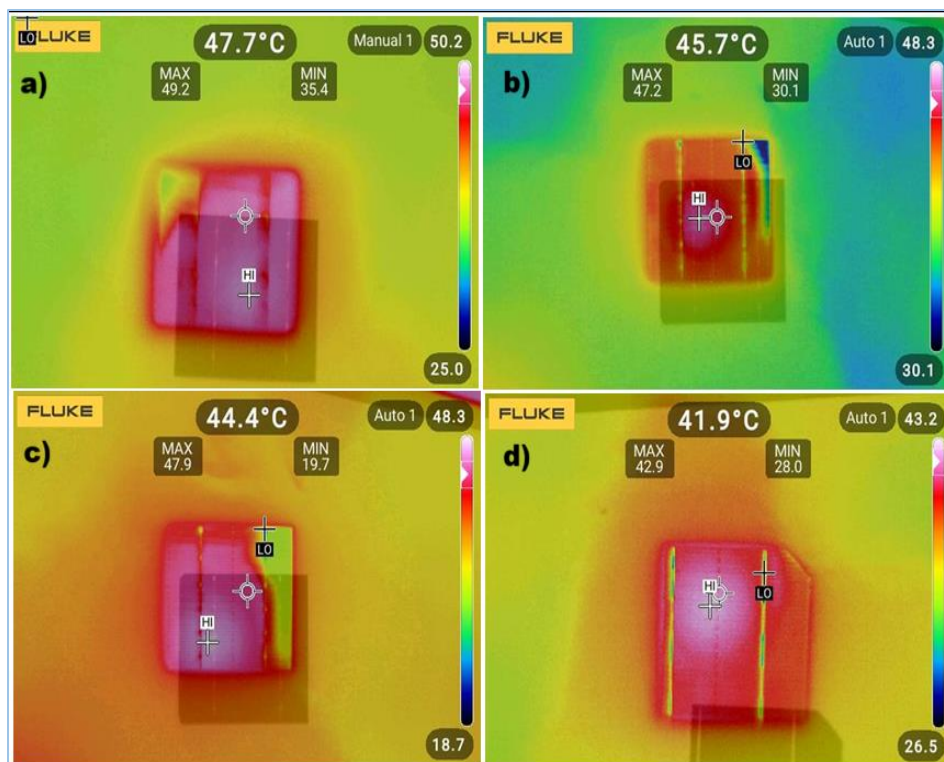


**Figure 8.** Thermal images of (a) bare, (b) SiO<sub>2</sub>, (c) VO<sub>2</sub> and (d) blended SiO<sub>2</sub>-VO<sub>2</sub> coated solar cells by electro-spraying under regulated light source.

The SiO<sub>2</sub> and VO<sub>2</sub> coated cell showed a minimum temperature of 45.7 °C and 44.4 °C, respectively. It might be due to larger effective surface area of the coated films as compare to the uncoated sample. This decreasing operating cell temperature of the coated samples can be attributed not only due to the influence of antireflection behavior alone. The SiO<sub>2</sub>-VO<sub>2</sub> coating also results in an increased light transmission, reduced non-radiative recombination loss and this limited the excess heat that could be produced within the cell. Moreover, the coating structure is homogeneous and finely-grained, which increases the quantity of the effective surface area, which is beneficial to thermal dissipation when illuminated. This decreases the internal heat generation and increases the heat spreading which in turn reduces the steady-state operating temperature [19]. Larger effective surface area leads to better cooling of the coated samples and hence SiO<sub>2</sub>-VO<sub>2</sub> coated films performance is significantly higher which might result in longer service life of the photo-voltic cells. The electro-spraying process of double layer coating of SiO<sub>2</sub>-VO<sub>2</sub> increased the power conversion efficiency of solar cell as confirmed by the structural, electrical, optical and thermal analysis.

#### 4. Conclusions

Using electro-spraying process, silicon dioxide and vanadium oxide were deposited as an anti-reflective coating on mono-crystalline solar cells. The SiO<sub>2</sub> and VO<sub>2</sub> were coated as a single material and also coated as a combined material that is blended SiO<sub>2</sub>-VO<sub>2</sub> on solar cells. The crystalline orientation of SiO<sub>2</sub> and VO<sub>2</sub> peaks were obtained using XRD. Using FESEM analysis, the cross-sectional view and thickness of the samples were found as 223 nm, 303 nm and 390 nm for SiO<sub>2</sub>, VO<sub>2</sub> and blended SiO<sub>2</sub>-VO<sub>2</sub> coated solar cells. The surface roughness of the samples was obtained by AFM investigation. Anti-reflection coating is primarily employed to reduce the reflection loss in photovoltaic cells. It is proved that the blended SiO<sub>2</sub>-VO<sub>2</sub> coated as AR coating on solar sample exhibited minimum reflectance of 6.55% as confirmed by UV-Vis spectroscopy analysis. Also, the

SiO<sub>2</sub>, VO<sub>2</sub> and SiO<sub>2</sub>-VO<sub>2</sub> coated cells showed a minimum resistivity of  $8.44 \times 10^{-3} \Omega \cdot \text{cm}$  and  $6.76 \times 10^{-3} \Omega \cdot \text{cm}$  compared to bare cell ( $9.23 \times 10^{-3} \Omega \cdot \text{cm}$ ). As resistivity reduces, the conductivity and photon to power conversion increases which ultimately leads to increased efficiency of solar cell. therefore, the blended SiO<sub>2</sub>-VO<sub>2</sub> coated cell with minimum resistivity exhibited the highest power conversion efficiency of 24.87%. This blended layer allows more photons to penetrate through the solar cells by reducing the light scattering. The temperature of the SiO<sub>2</sub>-VO<sub>2</sub> is also minimum which shows a correlation to the above results. The process of electro-spraying of SiO<sub>2</sub> and VO<sub>2</sub> as an anti-reflection coating on solar cells shows potential to increase the overall performance of solar cell, therefore rendering them sustainable in widespread applications.

**Acknowledgment:** The author is thankful to the Deanship of Scientific Research at Imam Mohammad Ibn Saud Islamic University (IMSIU), Riyadh, Saudi Arabia for supporting this research and for BIT, India for imaging support.

**Availability of Data and Materials:** The datasets used and analyzed during the current study are available from the corresponding author on reasonable request.

**Funding:** This research received no external funding.

**Author Contributions:** The single author had the sole role in designing, data collecting, analyzing, and writing the manuscript.

**Declaration of AI and AI-assisted Technologies in the Writing Process:** No AI tool used.

**Ethical Approval:** Not applicable.

**Conflict of Interest:** The author declares no conflict of interest.

## References

1. Dissanayake, K.; Kularatna-Abeywardana, D. A review of supercapacitors: Materials, technology, challenges, and renewable energy applications. *Journal of Energy Storage* 2024, 96, 112563. <https://doi.org/10.1016/j.est.2024.112563>
2. Zala, P.; Tripathi, B.; Khemnani, M.; et al. Optimizing anti-reflection coating using electrochemical impedance spectroscopy to enhance electrical performance of solar cell. *Optical and Quantum Electronics* 2025, 57(8), 452. <https://doi.org/10.1007/s11082-025-08371-1>
3. Singh, A.; Agarwal, P. Design and fabrication of anti-reflection coatings for its application in crystalline silicon solar cells. *Journal of Materials Science: Materials in Electronics* 2025, 36(12), 721. <https://doi.org/10.1007/s10854-025-14809-9>
4. Manzoor, S.; Filipič, M.; Onno, A.; et al. Visualizing light trapping within textured silicon solar cells. *Journal of Applied Physics* 2020, 127(6). <https://doi.org/10.1063/1.5131173>
5. Ayvazyan, G.; Dashtoyan, H.; Hakhoyan, L. Wide-range wavelength light scattering from black silicon layers: Profits for Perovskite/Si tandem solar cells. *physica status solidi (RRL)–Rapid Research Letters* 2025, 19(2), 2400235. <https://doi.org/10.1002/pssr.202400235>
6. Shanmugam, N.; Pugazhendhi, R.; Madurai Elavarasan, R.; et al. Anti-reflective coating materials: A holistic review from PV perspective. *Energies* 2020, 13(10), 2631. <https://doi.org/10.3390/en13102631>
7. Bock, N.; Dargaville, T.R.; Woodruff, M.A. Electro-spraying of polymers with the rapetic molecules: State of the art. *Progress in Polymer Science* 2012, 37(11), 1510–1551. <https://doi.org/10.1016/j.progpolymsci.2012.03.002>
8. Khanum, K.K.; Anakkavoor Krishnaswamy, J.; Ramamurthy, P.C. Design and fabrication of photonic structured organic solar cells by electro-spraying. *The Journal of Physical Chemistry C* 2017, 121(15), 8531–8540. <https://doi.org/10.1021/acs.jpcc.7b01698>
9. Okimura, K.; Mian, M.S.; Yamaguchi, I.; et al. High luminous transmittance and solar modulation of VO<sub>2</sub>-based smart windows with SiO<sub>2</sub> anti-reflection coatings. *Solar Energy Materials and Solar Cells* 2023, 251, 112162. <https://doi.org/10.1016/j.solmat.2022.112162>
10. Bocard, M.; Battaglia, C.; Haïnni, S.; et al. Multiscale transparent electrode architecture for efficient light management and carrier collection in solar cells. *Nano Letters* 2012, 12(3), 1344–1348. <https://doi.org/10.1021/nl203909u>

11. Wan, Y.; McIntosh, K.R.; Thomson, A.F. Characterisation and optimisation of PECVD SiN<sub>x</sub> as an antireflection coating and passivation layer for silicon solar cells. *AIP Advances* 2013, 3(3). <https://doi.org/10.1063/1.4795108>
12. Wang, C.; Zhao, L.; Liang, Z.; et al. New intelligent multifunctional SiO<sub>2</sub>/VO<sub>2</sub> composite films with enhanced infrared light regulation performance, solar modulation capability, and superhydrophobicity. *Science and Technology of Advanced Materials* 2017, 18(1), 563–573. <https://doi.org/10.1080/14686996.2017.1360752>
13. Jazaa, Y. Structural and efficiency analysis of polycrystalline Si cells with VO<sub>2</sub>-Si<sub>3</sub>N<sub>4</sub> antireflection coating. *Ceramics International* 2025, 51(24), 41037–41047. <https://doi.org/10.1016/j.ceramint.2025.06.329>
14. Jalali, A.; Vaezi, M.R.; Naderi, N.; et al. Investigating the effect of sol-gel solution concentration on the efficiency of silicon solar cells: Role of ZnO nanoparticles as anti-reflective layer. *Chemical Papers* 2020, 74, 253–260. <https://doi.org/10.1007/s11696-019-00872-0>
15. Hou, X.; Feng, J.; Ren, Y.; et al. Synthesis and adsorption properties of spongelike porous MnFe<sub>2</sub>O<sub>4</sub>. *Colloids and Surfaces A: Physicochemical and Engineering Aspects* 2010, 363(1–3), 1–7. <https://doi.org/10.1016/j.colsurfa.2010.03.016>
16. Maqsood, S.; Ishaq, M.; Ali, Z.; et al. Optimization of hydrophobic anti-reflection calcium fluoride films for ZnO/GaAs heterojunction solar cell: A simulation study. *Indian Journal of Physics* 2024, 98, 4919–4932. <https://doi.org/10.1007/s12648-024-03214-3>
17. Ali, K.; Khan, S.A.; Jafri, M.M. Effect of double layer (SiO<sub>2</sub>/TiO<sub>2</sub>) anti-reflective coating on silicon solar cells. *International Journal of Electrochemical Science* 2014, 9(12), 7865–7874. [https://doi.org/10.1016/S1452-3981\(23\)11011-X](https://doi.org/10.1016/S1452-3981(23)11011-X)
18. Wang, Z.; Liu, Z.; Hu, L.; et al. Experimental investigation on enhancing photovoltaic cell performance through synergistic radiative cooling and anti-reflection effects. *Case Studies in Thermal Engineering* 2025, 75, 107062. <https://doi.org/10.1016/j.csite.2025.107062>
19. Gunasekaran, R.; Kaliyannan, G.V.; Refaai, M.R.A.; et al. Sustainable manufacturing of 3D-Printed cyclic olefin copolymer coversheets with gahnite for enhanced silicon photovoltaic efficiency. *Ceramics International* 2025, 51(2), 2002–2013. <https://doi.org/10.1016/j.ceramint.2024.11.174>



© 2026 by the authors. Submitted for possible open access publication under the terms and conditions of the Creative Commons Attribution (CC BY) license (<http://creativecommons.org/licenses/by/4.0/>).